



Research articles

Impact of the magnitude of the magnetization on the induced anisotropy in transverse field annealed nanocrystalline cores



Athar Heddad^{a,b,*}, Hervé Chazal^a, Olivier Geoffroy^a, Alain Demier^c, Bashar Gony^b,
Thierry Waeckerlé^c, Sébastien Flury^a

^a Univ. Grenoble Alpes, CNRS, Grenoble INP, G2Elab, 38000 Grenoble, France

^b Aperam Alloys Amilly, 45200 Amilly, France

^c Aperam Alloys Imphy, 58160 Imphy, France

ARTICLE INFO

Keywords:

Finemet
Induced anisotropy
Field annealing
Memory effect
One step annealing
Field impact
Boosting effect
Shell model

ABSTRACT

We study the relation between the induced anisotropy obtained on nanocrystalline $Fe_{73.0}Cu_{4.1}Nb_{3.1}Si_{15.7}B_{7.1}$ toroidal cores crystallized under transverse field at 570 °C, and the polarization J_c of nanograins. To do this, an original disposition is used, mixing treated cores with cores made of electrotechnical SiFe alloy, featuring same geometry, using the interfacial magnetic charges to increase the field in treated cores. The field supplied by the coil being, playing on the proportion between treated and SiFe cores, effective field ranging between 33 mT and 230 mT were obtained inside treated cores. As a result, the induced anisotropy at the scale of the alloys at the end of crystallization range from $K_u = 12 \text{ J/m}^3$ to $K_u = 20 \text{ J/m}^3$.

To simulate the evolution of J_c during the crystallization process, the configuration of treated and SiFe cores in the sample holder was implemented in Altair FluxT FEM simulation environment with the dedicated polarization laws. Dealing with treated cores, the law $J_{cor}(H)$ at the scale of the core reflects the law $J_c(H)$ featured by nanograins during the crystallization process. $J_c(H)$ was modeled as a function of the crystallized fraction f_c .

The relation between the simulated J_c and the experimental final values of K_u/f_c (i.e. the anisotropy in nanograins) was then studied. This was done considering the polarization $\langle J_c \rangle$ averaged on the entire crystallization process, wondering about a possible memory effect.

1. Introduction

Finemet type nanocrystalline soft alloys exhibit vanishing effective anisotropy, allowing to induce coherent anisotropies by the mean of magnetic field annealing [1–4] or stress annealing [3–7]. We are interested here by transverse field annealing. Two variants can be processed, i.e. applying the field during the crystallization, (one step annealing, noted OSA in the following), or in a separate treatment (two steps annealing, noted TSA in the following) [2]. The mechanism usually invoked is the pair ordering [9,11], in the phase remaining magnetic at the annealing temperature T , i.e. SiFe nanograins, [2,8]. This effect has been put in evidence on bulk SiFe samples in [12,13]. According to the pair ordering model, the anisotropy K_u^c in the nanocrystallites should be controlled by T , which arbitrates the competition between magnetic (favorable) and chemical (unfavorable) ordering of the SiFe phase, as theoretically explained in [9] and [14]. K_u^c should also obey a J_c^2 dependency [10,11,15], J_c denoting the polarization of nanograins.

In partial contradiction with the pair ordering model, experiments show that, T given, the efficiency of the OSA is always superior to the TSA and the sensitivity of the efficiency to T is less pronounced for the TSA than for the OSA [2]. These observations did not receive clear interpretation, but, independently of the mechanism involved, this indicates that K_u^c is not determined by the final state only (TSA and OSA would feature same efficiency in this case). In other words, some memory effect exists, involving intermediate crystallization states. As a result, noting f_c^f the final value of the crystalline fraction f_c , one may expect a resulting anisotropy

$$K_u = \int_0^{f_c^f} K_u^c df_c,$$

where K_u^c is the anisotropy in nanograins in course of crystallization, assumed to include a f_c -dependent contribution, and K_u the final induced anisotropy, evaluated at the scale of the alloy.

In fact, in the range 480 °C < T < 580 °C usually practiced, Si_yFe_{1-y} nanograins experience a super-paramagnetic or weak coupling

* Corresponding author.

E-mail address: athar.heddad@g2elab.grenoble-inp.fr (A. Heddad).

regime [16,17], J_c depending on the size D of nanograins together with T , f_c , γ and the field H . This situation differs strongly from bulk crystalline alloys, where the local polarization is the spontaneous ferromagnetic polarization J_s^c , independently of H , except in the vicinity of the Curie temperature or in the case of intense annealing field (i.e. several Teslas). In the case of moderate field, the role of H in bulk crystalline alloys is so mostly to promote a uniform magnetization to obtain a coherent induced anisotropy at the scale of the core.

Accurate model of the weak coupling behavior has been published in [18,19]. According to this, the polarization experienced by nanograins may strongly vary during the crystallization. In this case, J_c^f , the final value of J_c , and $\langle J_c \rangle$, the mean value of the polarization experienced during the crystallization, will differ, and, according to the idea of a memory effect, it is more relevant to correlate K_u to $\langle J_c \rangle$ than to J_c^f . Crudely, assuming a power law, K_u should linearly depend on $\langle J_c^a \rangle$. Checking this idea is one of the goals we present here, the second one being to test an original arrangement of toroidal cores intended to boost the experienced field. We present this idea in the following part.

2. The boosting configuration

We need a panel of samples featuring a distribution of experienced polarizations and K_u as large as possible. The temperature profile has to be the same for all samples, to avoid parasitic effects in the interpretation of K_u distribution. The annealing temperature chosen was 570 °C, preceded by a ramp with slope 0.64 °C/min (cf. Fig. 5). The small value of the slope was chosen to smooth the exothermal pic corresponding to the crystallization of SiFe nanograins [20]. Annealings were achieved under Hydrogen atmosphere.

The distribution of mean polarizations $\langle J_c \rangle$ featured by samples is obtained playing on the field amplitude. A first point is to overcome the demagnetizing field H_j generated by the cores transversally magnetized (the subscript “j” indicates the magnetostatic origin of this contribution): we used Nanophy® cores made of wounded ribbons featuring composition $Fe_{73.0}Cu_{1.1}Nb_{3.1}Si_{15.7}B_{7.1}$ and thickness $20\mu m$, provided by Aperam Alloys Amilly, with internal and external radii $R_i = 10 mm$, $R_e = 15 mm$, and height $L = 10 mm$. The demagnetizing coefficient, calculated using FEM environment Altair FluxT (simply noted FluxT in the following), equals 0.36. Considering the limited field $\mu_0 H_a = 33 mT$ generated by the coil surrounding the furnace used in G2Elab, this would lead to unacceptable demagnetizing field. To null it, treated cores (in blue on Fig. 1a), are usually stacked together, and supplemented at each end by cores of same dimensions (in yellow), made of a wounded Electrotechnical SiFe sheet, to cancel magnetic charges at the edges. We improved this scheme, treated cores being interleaved with SiFe cores (cf. Fig. 1b), and define the dilution factor n as the number of SiFe cores separating two treated cores in a periodic configuration. The idea is that SiFe nanograins are super-paramagnetic or weakly coupled in course of annealing, treated cores featuring thus very low permeability ($\mu_r < 10$). In contrast, SiFe cores exhibit ferromagnetic behavior with high permeability belong saturation knee as long as $T < T_C \cong 746$ °C. This means that the field inside SiFe cores is negligible or, in other words, that the field \vec{H}_j due to polarizations (in red on Fig. 1b) cancels \vec{H}_a (in black) inside SiFe cores and so reinforces H inside treated cores. As a result, SiFe cores will be called boosting cores in the following. Given n , one obtains by this way

$$H \cong (n + 1)H_a \quad (1)$$

Playing on the dilution factor, $0 \leq n \leq 6$, we obtain the field magnitudes range $33 mT \leq \mu_0 H \leq 230 mT$, leading to a panel of treated cores having experienced different profiles of magnetization in the course of crystallization.

We finally underline another advantage of the interleave, i.e. the role of radiators played by boosting cores, allowing to smooth even better the exothermal peak mentioned above.

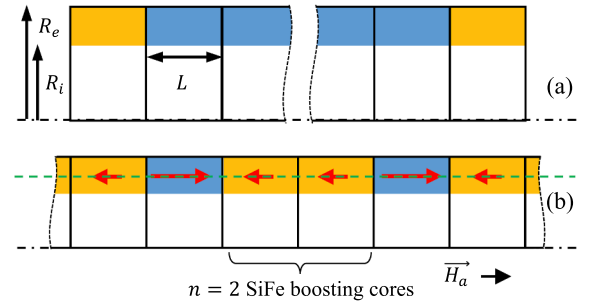


Fig. 1. (a): classical configuration of treated cores (in blue) to cancel demagnetizing field. (b): Use of SiFe boosting cores to reinforce the field inside treated cores. Red arrows represent the field \vec{H}_j generated by polarizations, demagnetizing inside boosting cores, magnetizing inside treated cores. Arrows are plotted along the green line used to calculate mean values (cf. Section 5).

3. Experimental results

K_u is experimentally determined by a surface measurement, as illustrated on [21], Fig. 1. We underline the difference in the limiting curve we have chosen, compared to [22], considering that a part of the surface enclosed in [22] is due to dissipative contributions and so not related to stored energy. The efficiency of the interleaved boosting configuration is illustrated on Fig. 2, looking to the evolution of K_u with respect to n , for cores located in the middle part of stacks, representative of an ideal periodic arrangement.

The interleaved configuration permits so to circumvent limitations of coils, despite the dilution effect, unfavourable from an industrial point of view. At least, this experiment allows to determine experimentally the amplitude of the resulting K_u obtained for given H , approximately indicated by (1), independently of the way used to produce it.

The accurate simulation of equilibriums corresponding to the interleaved configuration will allow to check the validity of (1) and provide additional information dealing with the homogeneity of field, edges effects due to the finite size of stacks... and the resulting polarizations, crucial point dealing with the dependency relation $K_u^c(\langle J_c \rangle)$ we aim to study! This is the subject of the following part.

4. Simulation of polarization in course of crystallization

The simulation of equilibrium magnetizations involves different scales, pictured on Fig. 3: the last one deals with homogeneous cores, implemented in FluxT, together with SiFe boosting cores, in the interleaved configuration discussed above. The equilibrium polarizations are solved knowing the corresponding magnetization laws, $J_{cor}(H)$ and $J_{Bcor}(H)$, respectively related to treated and boosting cores.

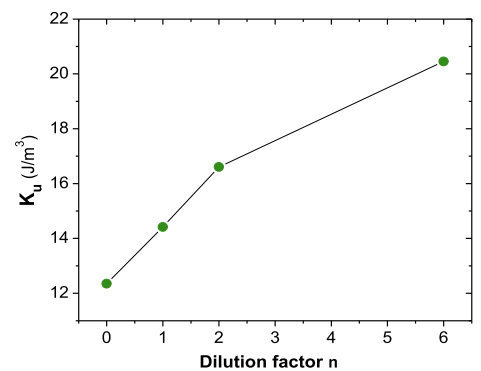


Fig. 2. Evolution of K_u with respect to the dilution factor n for given applied field. $\mu_0 H_a = 33 mT$.

Unfortunately, the weak coupling regime experienced by SiFe nanograins at annealing temperature does not allow easy experimental characterization of $J_{cor}(H)$, because of the very high field amplitude required but mostly because the intermediate states of crystallisation are totally unstable at the annealing temperature. We will so determine $J_{cor}(H)$ in course of crystallization by the mean of modelling.

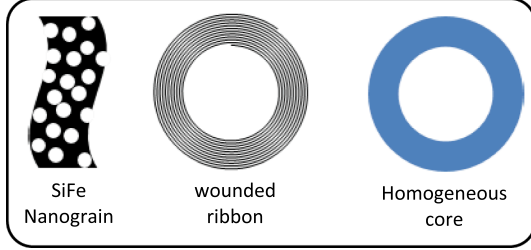


Fig. 3. The different scales involved related to treated cores.

To do it, it is necessary to come back to the finest scale, i.e. the SiFe nanograin: As detailed in [18,19], the polarization of a nanograin obeys

$$\frac{J_c}{J_s^c} = \mathcal{L} \left[\frac{J_s^c \pi D^3 f_c J_c / (3\mu_0) + H}{6k_B T} \right] \quad (2)$$

where \mathcal{L} denotes the Langevin function, J_s^c the spontaneous ferromagnetic polarization of the Si_yFe_{1-y} phase, itself depending on y and T , and S a screening coefficient introduced in the frame of the “shell model” [18,19]. It means that the law $J_c(H)$ in the course of crystallization is determined by the evolution of quadruplet (T, y, f_c, D) . We'll so now investigate this point.

4.1. Evolution of crystallographic parameters in the course of crystallization

We use the data bases performed at the Aperam Imphy Center Research on samples featuring the same composition than in the present case. Isothermal crystallisations were studied by X ray diffraction, allowing to obtain analytical laws $f_c(T, t)$, $D(f_c, T)$, $y(f_c)$ [19]. The case of f_c is illustrated on Fig. 4. Analytical expression $\partial f_c(T, t)/\partial t$ is easily derived. In our context, T depends on time t , as shown on Fig. 5 (green curve). We so re-integrate, accounting at this stage from the dependency relation $T(t)$, i.e.

$$f_c(t) = \int_0^t \frac{\partial f_c(T(t), t)}{\partial t} dt$$

The resulting $f_c(t)$ curve is plotted in blue on Fig. 5.

Evolution of parameters Dandy are obtained in a similar way and are plotted on the same figure. The maximum on the $y(t)$ curve corresponds to the entrance in the regime of total diffusion of available Si in

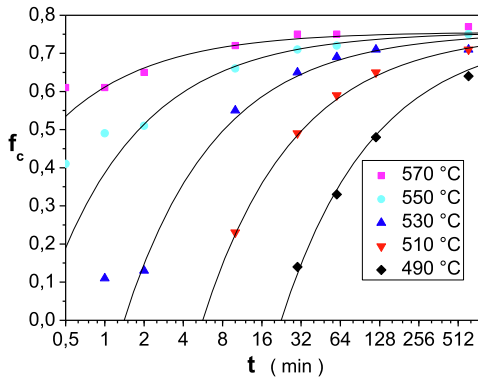


Fig. 4. Evolution of f_c in course of isothermal annealings (with the courtesy of Aperam Imphy Research Centre). Analytic curves are superimposed to measured points.

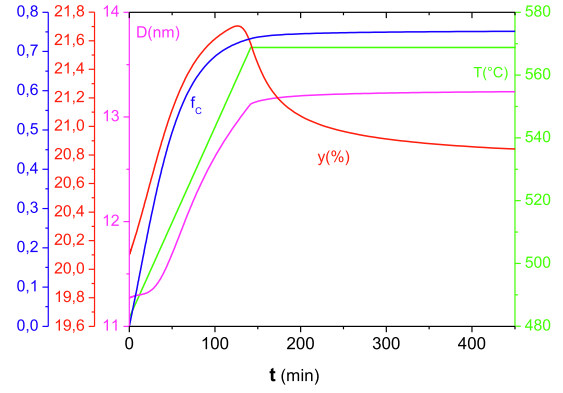


Fig. 5. Evolution of parameters f_c , D , y during annealing, given the temperature profile $T(t)$ (in green). The origin of time is taken at the beginning of crystallisation.

the SiFe phase, obtained for $f_c \cong 0.7$ [19,20]: from this point, the increase of f_c implies a decrease of y (we illustrate this behaviour on Fig. 6, dealing with a separate experiment concerning samples featuring same alloy composition than in the present case, annealed during one hour at different temperatures).

D varying between 11 – 13nm, and y between 20 – 22%, the most sensitive parameters are f_c and T .

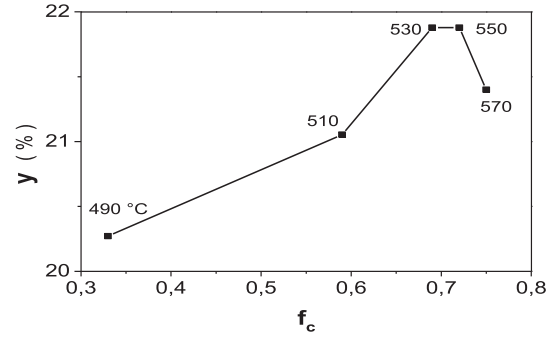


Fig. 6. Evolution of composition of nanograins, vs f_c , for $Fe_{73.0}Cu_{4.1}Nb_{3.1}Si_{15.7}B_{7.1}$ samples annealed during one hour at different temperatures. Samples are characterized by X ray diffraction (with the courtesy of Aperam Imphy Research Centre).

The quadruplets T, y, f_c, D being known at any time, the use of (2) allows to determine the magnetic law $J_c(H, f_c)$ for any value of f_c . Owing the impact of J_s^c on $J_c(H, f_c)$ indicated by (2), we detail the laws $J_s^c(T, y)$:

4.2. The spontaneous ferromagnetic polarization $J_s^c(T, y)$

According to [23,19], SiFe alloys obey a Heisenberg type magnetothermic behaviour for $600K < T < T_C$, i.e.

$$J_s^c(T) = {}^{600}J_s^c \left(\frac{T_C - T}{T_C - 600} \right)^{0.36} \quad (3)$$

$J_s^c(T)$ is determined for any composition y knowing the relations $T_C(y)$ and ${}^{600}J_s^c(y)$. Compiling data from [24–26], and our own characterizations [21], we adjust in the range $0 < y < 0.25$ the analytical formulations:

$$T_C = 1044, 6 - 288, 5y - 3825y^2 + 6059y^3 \quad (4)$$

$${}^{600}J_s^c = 1, 99; -; \backslash; 3, 89; y; -; \backslash; 0, 229; y^2 \quad (5)$$

From (3)–(5), we obtain the curves plotted on Fig. 7, relative to the different compositions related to eight sampled values of f_c . The points

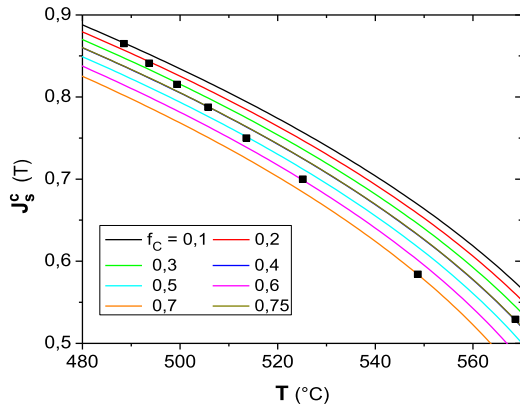


Fig. 7. Evolution of the spontaneous ferromagnetic polarization in course of crystallization. The eight thermomagnetic curves correspond to the compositions of the nanocrystalline phase associated to the values of f_c sampled (curves $f_c = 0.4$ and $f_c = 0.75$ are superimposed, corresponding to the same y value).

correspond to the annealing profile.

4.3. Magnetization laws

$J_s^c(f_c)$ known, $J_c(H, f_c)$ curves are plotted on Fig. 8. They show a complex behaviour, the curves crossing each other. Their relative positions for high values of H is easy to understand, given the fact that J_s^c decreases with increasing f_c , as shown by Fig. 7. For low values of H , f_c influences the argument of the Langevin function in (2), and counterbalances the effect of the decrease of J_s^c , accounting so for the higher values of J_c with increasing f_c at the beginning of curves. Lastly, curves corresponding to $f_c = 0.7$ and 0.75 seem to be separated from others, simply because for $y \cong 0.21$, representative of the composition of SiFe nanograins, T_c is around 600 °C [19,24], in the vicinity of the final annealing temperature (570 °C). For comparison, Figs. 5 or 7 indicates that $f_c = 0.6$ is obtained for $T = 525^\circ\text{C}$.

From the curves of Fig. 8, one obtains the magnetization laws $J_{cor}(H, f_c)$ by simple dilution operations, ie

$$J_{cor}(H, f_c) = k f_c J_c(H, f_c) \quad (6)$$

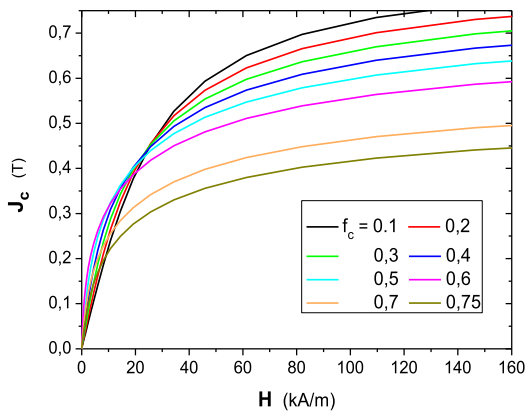


Fig. 8. Some iso f_c magnetic laws $J_c(H)$ featured by nanograins.

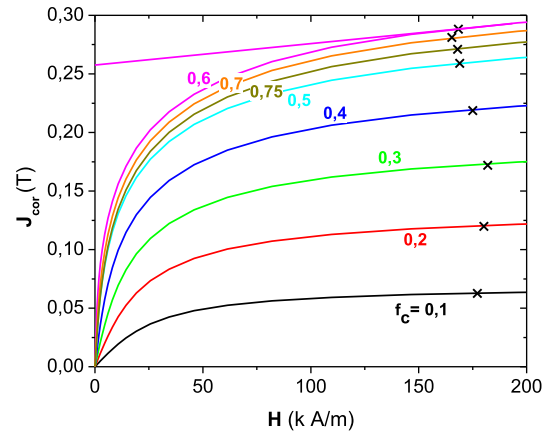


Fig. 9. The magnetic laws $J_{cor}(H)$ corresponding to homogeneous cores implemented on FluxT. The crosses indicate the operating points corresponding to the dilution factor. $n = 6$.

$k \cong 0.8$ denotes the filling factor resulting from the wounding process. Resulting curves are plotted on Fig. 9.

The same has to be done for the “boosting” SiFe cores. This is much easier, because they are ferromagnetic at the annealing temperatures and so easy to characterize experimentally. Measured points are plotted on Fig. 10 in the interesting range for different relevant temperatures. Generic analytical formulations are adjusted (superimposed on experimental points), with parameters built as functions of T , allowing to obtain magnetization laws at any temperature in the range [480 °C, 600 °C]. Corresponding laws $J_{Bcor}(H, T) = k' J_{SiFe}(H, T)$ are implemented in FluxT, with $k' = 0.93$ the relevant dilution coefficient, together with $J_{cor}(H, f_c)$ laws indicated by (6).

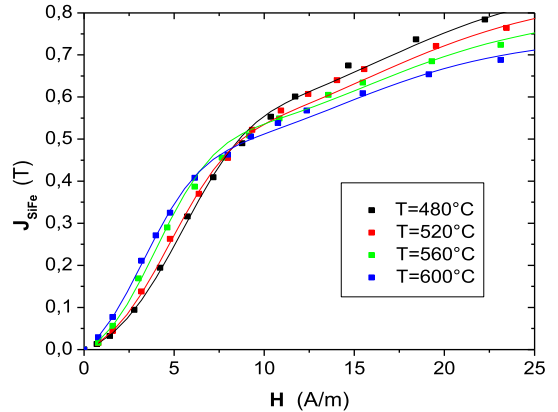


Fig. 10. The $J_{SiFe}(H)$ curves corresponding to the boosting cores alloy (Electrotechnical steel) for different relevant temperatures. The analytical adjusted laws are superimposed (continuous lines).

From now on, equilibrium polarizations and fields are available for any value of f_c sampled, provided that the topology of the arrangement is properly described, including so the finite size of stacks to account for edges effects. A point subject to discussion is the value of the representative air-gap e to be introduced between neighboring cores in

the description. In doubt, we simulated with $e = 50\mu m, 100\mu m, 200\mu m$. The simulated results are nearly insensitive to the value, as one could predict owing to the very low permeability featured by treated cores, as shown by the slope reported on curve $J_{cor}(H, f_c = 0.6)$ on Fig. 9, indicating a differential susceptibility around 0.15 at the operating point. The results we indicate in the following were obtained introducing $e = 100\mu m$.

5. Simulated results

Dealing with the boost effect, Fig. 11 represents the field in a treated core along the line plotted in green in Fig. 1b.

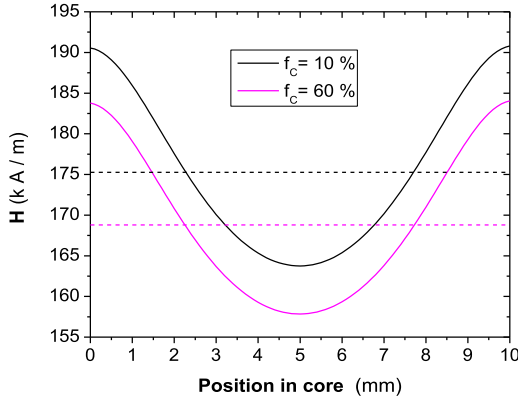


Fig. 11. Profile of the field inside treated core in the central part of the stack for the dilution factor $n = 6$ and two different values of f_c . H is calculated along the green line pictured on Fig. 1b.

The cases chosen for illustrating are $n = 6$, with $f_c = 0.1; 0.6$. The mean values H_{mea} are indicated in dashed together. They correspond to the crosses reported on Fig. 9 for those two cases. H_{mea} , around 172kA/m , is 7% less than the value predicted by (1), and the relative inhomogeneity $\Delta H = 0.5(H_{max} - H_{min})/H_{mea}$ is around 9%. Giving the fact that the working points are in the asymptotic part of the curves, the resulting magnetization inhomogeneity is in fact much less, i.e. $\Delta J \cong 0.9\%$. The inhomogeneity remains negligible even for lower dilution factor, with $\Delta J (n = 2) \cong 1.6\%$.

Dealing with polarizations, the values returned by FluxT concern the homogeneous cores. They are plotted on Fig. 12, related to treated cores located in the center parts of stacks. The values obtained for $n = 6$

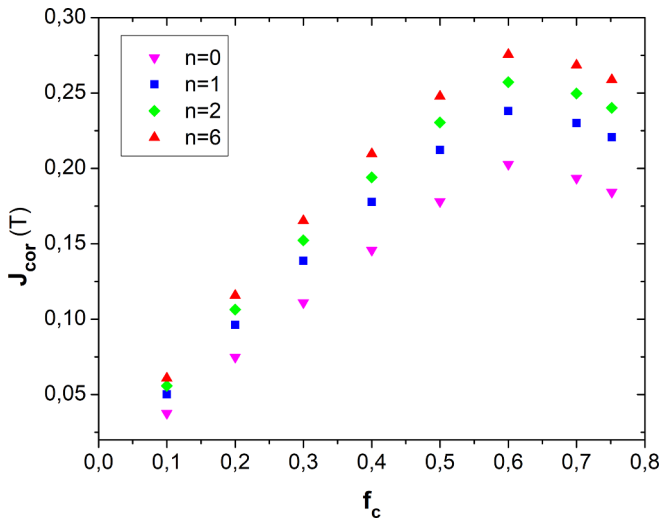


Fig. 12. Equilibrium polarizations featured by treated cores (central part of the stacks) in course of polarization for different dilution factors.

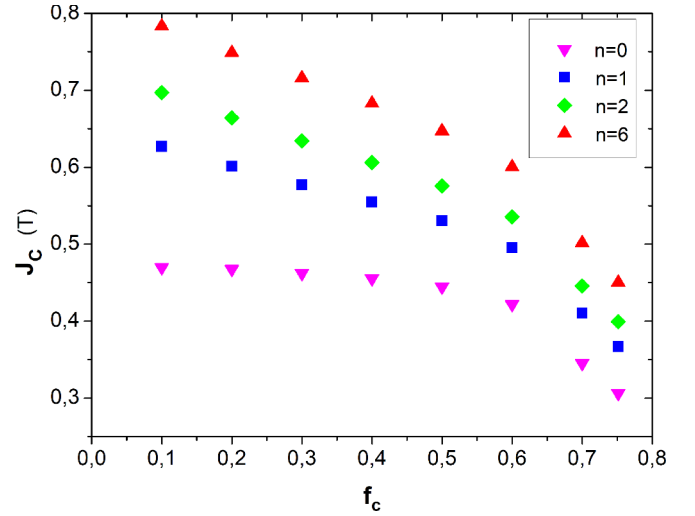


Fig. 13. Equilibrium polarizations featured by nanograins in course of polarization. The curves correspond to those of Fig. 12.

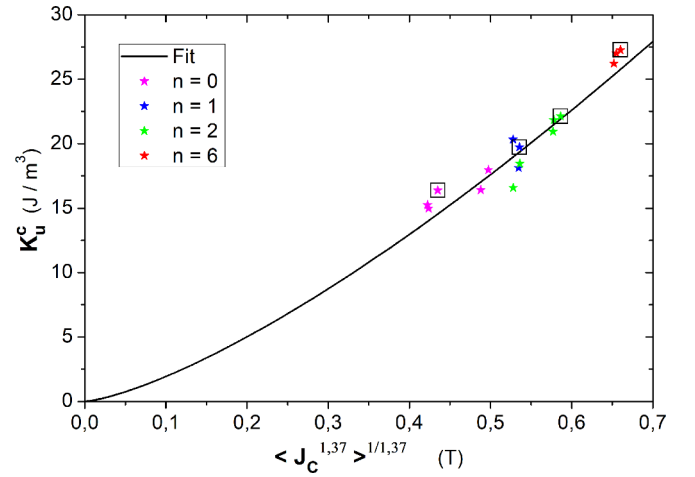


Fig. 14. Induced anisotropy $K_u^c = K_u/f_c^f$ in nanograins at the end of annealing, vs mean polarizations experienced in course of crystallization. The points surrounded are those illustrating Fig. 2.

(in red, maximum dilution factor) correspond to the crosses on the curves of Fig. 9. One notices that the curves feature a maximum value for $f_c = 0.6$ instead of $f_c = 0.75$, as one could expected looking only for the dilution effect, for the reason already discussed in the context of Fig. 8 (vicinity of T_c for the highest values of f_c).

Dealing with the induced anisotropy, we are interested by the polarization featured by nanocrystals. We so use (6) to obtain $J_c(f_c)$ from $J_{cor}(f_c)$ returned by FluxT. The curves are plotted on Fig. 13. The monotonous decrease featured by J_c with increasing f_c is again due to the increasing temperature, with the expected abrupt fall towards the highest values of f_c due to the vicinity of T_c . Comparing the curves between them in the range $f_c < 0.6$, we notice that the absolute values of slopes decrease when n decreases. This is due to the fact that H decreasing too, the influence of f_c in the argument of the Langevin function discussed in the beginning of §4.3 is more and more visible, counter-balancing partially the effect of T .

6. Relation $K_u^c(\langle J_c \rangle)$

We performed four different dilution factors. Due to finite sizes of stacks, only the central parts of them experienced the field amplitude expected considering an ideal periodic scheme. The corresponding

samples were chosen to illustrate Figs. 2, 11–13. They are distinguished on Fig. 14.

The field amplitude being not uniform along a stack, this explains the spread of simulated polarizations, improving the distribution of points.

Whereas the pair model provides for an exponent equal to two, the fit illustrated on Fig. 14 indicates $K_u^c \propto \langle J_c^{1.37} \rangle$. This significant deviation in the exponent values suggests that a different mechanism operates, together with the pair model, responsible for the memory effect discussed in the introduction.

7. Conclusions and perspectives

The efficiency of the interleaved configuration has been clearly evidenced, regarding the amplification of field experienced by the treated cores and the resulting increase of the induced anisotropy amplitude illustrated on Fig. 2.

Dealing with the interpretation of the improved efficiency of the TSA compared to the OSA, a limitation of the very preliminary study reported here is that we wonder on a memory effect, but we only have the final value of induced anisotropy to support our thinking. Measurement of K_u on interrupted anneals would offer precious additional information on intermediate states. To do this, it is necessary to cool abruptly for stopping efficiently the crystallization process. For this, samples have to be extracted in a cold zone of the furnace. In the same time, the field must be maintained until complete cooling to preserve the K_u^c value corresponding to the moment the crystallization was interrupted. We so need additional coil located around the cold zone. We improve now our furnace for this purpose.

CRediT authorship contribution statement

Athar Heddad: Methodology, Formal analysis, Investigation, Visualization, Software. **Hervé Chazal:** Methodology, Formal analysis, Investigation. **Olivier Geoffroy:** Conceptualization, Methodology, Formal analysis, Validation, Writing - review & editing. **Alain Demier:** Resources, Investigation. **Bashar Gony:** Resources, Project administration, Funding acquisition. **Thierry Waeckerlé:** Supervision, Resources, Project administration, Funding acquisition. **Sébastien Flury:** Resources, Investigation.

Declaration of Competing Interest

The authors declare that they have no known competing financial interests or personal relationships that could have appeared to influence the work reported in this paper.

Acknowledgment

This study was partially supported by “Association Nationale de la Recherche et de la Technologie.” (convention CIFRE 2018/1308).

References

- [1] Y. Yoshizawa, K. Yamauchi, Effects of magnetic field annealing on magnetic properties in ultrafine crystalline Fe-Cu-Nb-Si-B alloys, *IEEE Trans. Mag.* 25 (1989) 3324–3326.
- [2] G. Herzer, Magnetic field-induced anisotropy in nano-crystalline Fe-Cu-Nb-Si-B alloys, *J. Mag. Magn. Mat.* 133 (1994) 248–250.
- [3] C. Migue, A. Zhukov, J.J. del Val, J. Gonzalez, Coercivity and induced magnetic anisotropy by stress and/or field annealing in Fe- and Co-based (Finemet-type) amorphous alloys, *J. Mag. Magn. Mat.* 294 (2005) 245–251.
- [4] R. Madugndo, O. Geoffroy, T. Waeckerlé, B. Frincu, S. Kodjikian, S. Rivoirard, Improved soft magnetic properties in nanocrystalline FeCuNbSiB Nanophy® cores by intense magnetic field annealing, *J. Mag. Magn. Mat.* 422 (2017) 475–478.
- [5] F. Alves, F. Simon, S.N. Kane, F. Mazaleyrat, T. Waeckerlé, T. Save, A. Gupta, Influence of rapid stress annealing on magnetic and structural properties of nanocrystalline Fe74.5Cu1Nb3Si15.5B6 alloy, *J. Mag. Magn. Mat.* 294 (2005) e141–e144.
- [6] T. Waeckerlé, T. Save, A. Demier, New stressed and continuously annealed low μ nanocrystalline FeCuNbSiB cores for watt-hour-metering or differential mode inductance applications, *J. Mag. Magn. Mat.* 320 (2008) e797–e801.
- [7] G. Herzer, V. Budinsky, C. Polak, Magnetic properties of FeCuNbSiB nanocrystallized by flash annealing under high tensile stress, *Phys. Stat. Solidi B* 248 (2011) 2382–2388.
- [8] P.R. Ohodnicki, M.E. McHenry, D.E. Laughlin, Monte Carlo studies of directional pair ordering in disordered binary and ternary ferromagnetic BCC crystalline alloys, *J. Appl. Phys.* 101 (9) (2007) 09N118, <https://doi.org/10.1063/1.2711389>.
- [9] L. Néel, Anisotropie superficielle et surstructures d'orientation magnétique, *J. Phys. Radium* 15 (1954) 225.
- [10] J.C. Slonczewski, Magnetic annealing, in: G.T. Rado, H. Suhl (Eds.), *Magnetism*, New York Academic Press, 1966.
- [11] R. O' Handley, *Modern Magnetic Materials. Principles and Applications*, John Wiley and Sons, 2000.
- [12] K. Sixtus, Anisotropie in Eisen-Einkristallen nach Glühen im Magnetfeld, *Z. Angew. Phys.* 28 (1970) 270–274.
- [13] M. Goertz, Iron-silicon alloys heat treated in a magnetic field, *J. Appl. Phys.* 22 (1951) 964–965.
- [14] T. Iwata, Statistical thermodynamics of binary solid solutions with anisotropic distribution of atoms, *Sci. Rep. Research Inst. Tohoku Univ. Ser. A10* (34) (1958) 34–50.
- [15] P.R. Ohodnicki, J. Long, D.E. Laughlin, M.E. McHenry, V. Keylin, J. Huth, Composition dependence of field induced anisotropy in ferromagnetic (Co, Fe₈₉Zr₇B₄ and (Co, Fe₈₈Zr₇B₄Cu₁ amorphous and nanocrystalline ribbons, *J. Appl. Phys.* 104 (2008) 113909.
- [16] G. Herzer, Soft magnetic nanocrystalline materials, *Script. Met. Mater.* 33 (1995) 1741–1756.
- [17] F. Mazaleyrat, L.K. Varga, Thermo-magnetic transitions in two-phase nanostructured materials, *IEEE Trans. Magn.* 37 (2001) 2232–2234.
- [18] O. Geoffroy, H. Chazal, Y. Yao, T. Waeckerlé, J. Roudet, Modelization of superferromagnetism in soft nanocrystalline materials based on an accurate description of magnetostatic interactions, *IEEE Trans. Magn.* 50 (2014) 1–4.
- [19] N. Boust, O. Geoffroy, H. Chazal, S. Flury, T. Waeckerlé, A. Demier, B. Gony, J. Roudet, Use of superparamagnetic temperature transition measurement in nanocrystalline alloys to determine low crystalline fractions by modeling of the weak-coupling behavior, *J. Mag. Magn. Mat.* 478 (2019) 122–131.
- [20] G. Herzer, Nanocrystalline soft magnetic alloys, *Buschow, Handbook Magn. Mater.* 10 (1997).
- [21] N. Boust, O. Geoffroy, H. Chazal, J. Roudet, Modeling of hysteresis in FeCuNbSiB cores with transverse Ku, *IEEE Trans. Magn.* 53 (2017) 7301104.
- [22] S. Florer, G. Herzer, Random and uniform anisotropy in soft magnetic nanocrystalline alloys, *J. Mag. Magn. Mat.* 322 (2010) 1511–1514.
- [23] G. Herzer, Grain structure and magnetism of nanocrystalline ferromagnets, *IEEE Trans. Magn.* 25 (1989) 3327–3329.
- [24] M. Fallot, *Ferromagnétisme des Alliages de fer*, Phd thesis, faculté des sciences de l'université de Strasbourg, 1934.
- [25] R. Becker, W. Döring (Eds.), *Ferromagnetismus*, Springer Berlin Heidelberg, Berlin, Heidelberg, 1939.
- [26] T. Shinjo, Y. Nakamura, N. Shikazono, Magnetic study of Fe3Si and Fe5Si3 by Mössbauer effect, *J. Phys. Soc. Jpn.* 18 (1963) 797.